

Geophysical Research Letters[®]

RESEARCH LETTER

10.1029/2021GL097595

[†]Deceased 15 April 2022.

Key Points:

- Multiyear sea ice (MYI) area loss in the Beaufort Sea quadrupled from 46,000 km²/yr⁻¹ in 1997–2001 to 183,000 km²/yr⁻¹ in 2017–2021
- MYI area loss peaked at 385,000 km² in 2018, which is close to the annual MYI area export through Fram Strait
- The Beaufort Sea has become a MYI export pathway rivaling the Fram Strait, encouraging the pan-Arctic transition to a seasonal ice cover

Supporting Information:

Supporting Information may be found in the online version of this article.

Correspondence to:

D. G. Babb,
david.babb@umanitoba.ca


Citation:

Babb, D. G., Galley, R. J., Howell, S. E. L., Landy, J. C., Stroeve, J. C., & Barber, D. G. (2022). Increasing multiyear sea ice loss in the Beaufort Sea: A new export pathway for the diminishing multiyear ice cover of the Arctic Ocean. *Geophysical Research Letters*, 49, e2021GL097595. <https://doi.org/10.1029/2021GL097595>

Received 22 DEC 2021

Accepted 7 APR 2022

Increasing Multiyear Sea Ice Loss in the Beaufort Sea: A New Export Pathway for the Diminishing Multiyear Ice Cover of the Arctic Ocean

David G. Babb¹ , Ryan J. Galley^{2,3}, Stephen E. L. Howell⁴ , Jack C. Landy⁵ ,
Julienne C. Stroeve^{1,6,7} , and David G. Barber^{1,†} 

¹Centre for Earth Observation Science, University of Manitoba, Winnipeg, MB, Canada, ²Department of Environment and Geography, University of Manitoba, Winnipeg, MB, Canada, ³Department of Fisheries and Oceans Canada, Winnipeg, MB, Canada, ⁴Environment and Climate Change Canada, Toronto, ON, Canada, ⁵Department of Physics and Technology, UiT The Arctic University of Norway, Tromsø, Norway, ⁶CPOM, London, UK, ⁷NSIDC, Boulder, CO, USA

Abstract Historically, multiyear sea ice (MYI) covered a majority of the Arctic and circulated through the Beaufort Gyre for years. However, increased ice melt in the Beaufort Sea during the early 2000s was proposed to have severed this circulation. Constructing a regional MYI budget from 1997 to 2021 reveals that MYI import into the Beaufort Sea has increased year-round, yet less MYI now survives through summer and is transported onwards in the Gyre. Annual average MYI loss quadrupled over the study period and increased from ~7% to ~33% of annual Fram Strait MYI export, while the peak in 2018 (385,000 km²) was similar in magnitude to Fram Strait MYI export. The ice-albedo feedback coupled with the transition toward younger thinner MYI is responsible for the increased MYI loss. MYI transport through the Beaufort Gyre has not been severed, but it has been reduced so severely to prevent it from being redistributed throughout the Arctic Ocean.

Plain Language Summary Historically, sea ice grew thicker and aged into multiyear sea ice (MYI) as it was transported clockwise around the Beaufort Gyre for up to and beyond 10 years. This pattern facilitated the pan-Arctic distribution of MYI that was typical of the 1980s and 1990s. However, warming temperatures and greater sea ice melt in the Beaufort Sea since the early 2000s have significantly increased the annual area of MYI lost to melt and was proposed to have severed MYI transport through the Beaufort Gyre. Here, we use a regional MYI budget to show that an increasing area of MYI is lost annually in the Beaufort Sea and that this has considerably altered and interrupted MYI transport through the Gyre for prolonged periods during recent years. This change has implications regionally for wildlife, shipping, and local communities, while also having an effect on the resiliency of the pan-Arctic ice pack.

1. Introduction

Multiyear sea ice (MYI) comprises the thickest and most robust sea ice in the Arctic; however, its extent is declining as the Arctic transitions to a predominantly seasonal ice cover (Figure 1; Kwok, 2018). During the 1950s and 1960s, MYI covered the vast majority of the Arctic Ocean (~5.5 × 10⁶ km²; Nghiem et al., 2007) and grew thicker as it circulated through the anticyclonic Beaufort Gyre for up to and beyond 10 years (Rigor & Wallace, 2004). Within the Gyre, MYI is transported from the central Arctic, where the thickest and oldest ice is compressed against the northern coast of Greenland and the Canadian Arctic Archipelago (CAA; Bourke & Garret, 1987; Kwok, 2015), through the Beaufort and Chukchi Seas, then onward to the Eastern Arctic. From there MYI is circulated northwards and either retained and recirculated within the Gyre or entrained in the Transpolar Drift Stream and exported through the Fram Strait (Figure 1). The retention of MYI within the Gyre is a critical factor in the mass balance of the Arctic Ocean, as it redistributes MYI throughout the Arctic, maintaining the pan-Arctic distribution of MYI observed throughout the second half of the twentieth century (Nghiem et al., 2007) and the start of the observational record in the 1980s (Figure 1a; Maslanik et al., 2011). MYI survival through the Beaufort Sea is key to the process of MYI redistribution because the Beaufort serves as a conduit connecting the central Arctic to the Eastern Arctic. Maslanik et al. (2011) showed that between 1981 and 2005, 93% of MYI in the Beaufort Sea survived through summer, which thereby fostered the redistribution of MYI through the Gyre.

In 1998, the Beaufort Sea transitioned to a thinner state following anomalous atmospheric forcing and record ice loss (Hutchings & Rigor, 2012; Maslanik et al., 1999). Since then increased solar heating of the upper ocean

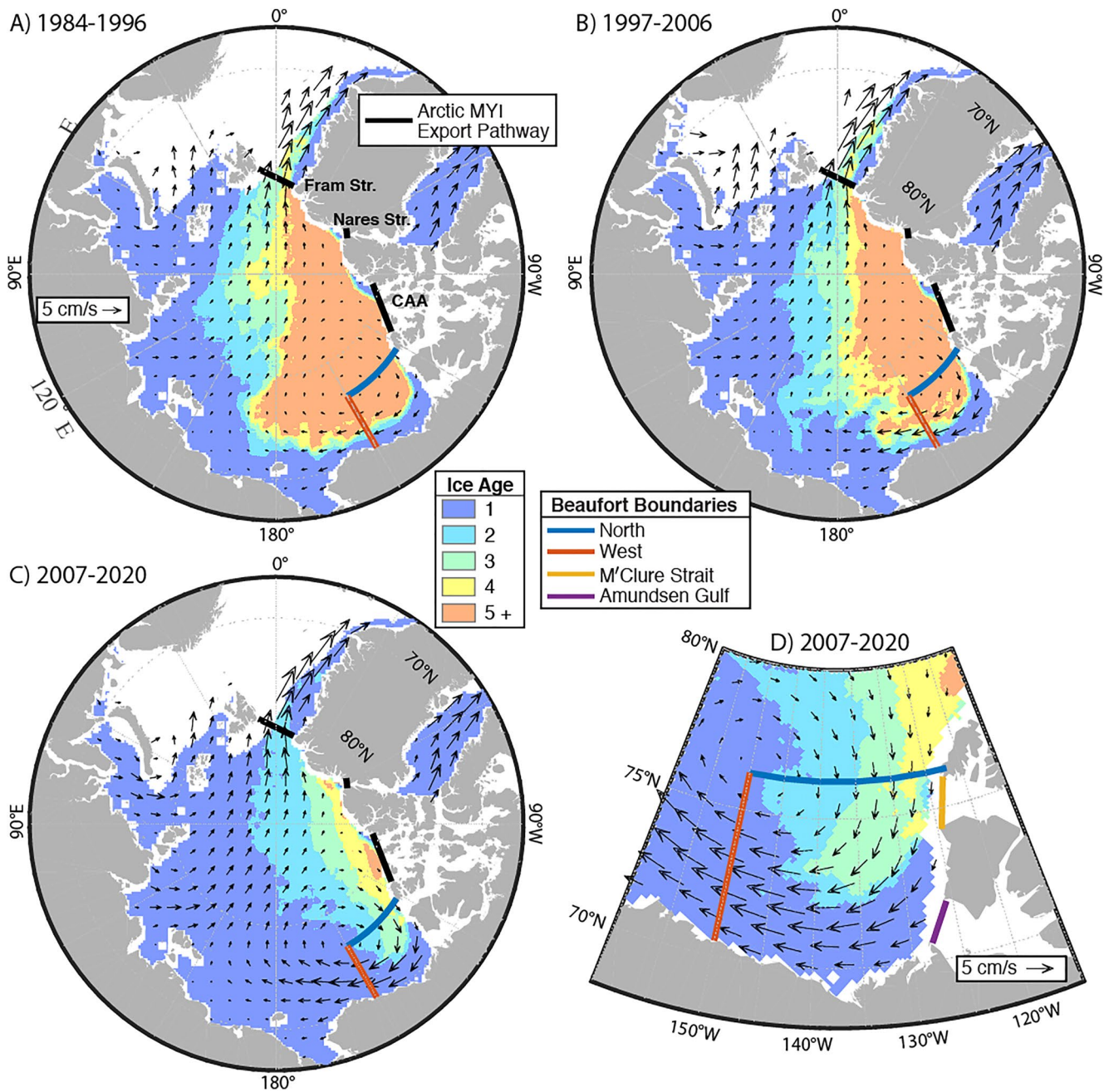


Figure 1. (a–c) Pan-Arctic fields of mean annual sea ice motion and median ice age during April between 1984–1996, 1997–2006, and 2007–2020. The northern and western boundaries of the Beaufort Sea and other MYI export pathways are presented. (d) Mean annual sea ice motion and median ice age during April in the Beaufort Sea from 2007 to 2020, with the four boundaries of the Beaufort denoted.

and heat transport through the Bering Strait have increased sea ice melt throughout the western Arctic (Planck et al., 2020; Woodgate et al., 2010), particularly bottom melt, of which an extreme amount (2 m) was observed on an MYI floe in the Beaufort Sea during 2007 (Perovich et al., 2008). Increased ice melt within the Beaufort Sea has led to reduced summer sea ice extent (Babb et al., 2019), year-round reductions in MYI area (Galley et al., 2016), reductions in MYI thickness (Krishfield et al., 2014), and increased MYI loss, which increased through the 2000s to a peak in 2008 (Kwok & Cunningham, 2010). Ultimately, the survival rate of MYI passing through the Beaufort Sea decreased from 93% between 1981–2005 to 73% between 2006 and 2010 (Maslanik et al., 2011), a change that was further emphasized by the complete loss of the regional MYI pack during summer

in 2010, 2012, and 2016 (Babb et al., 2016, 2019; Stroeve et al., 2011). However, regardless of MYI loss during summer, the Beaufort Sea continues to be resupplied with MYI from the central Arctic via the Gyre (Figure 1; Babb et al., 2020; Galley et al., 2016; Howell et al., 2016), though less of it is likely to survive through summer. As a result, younger ice is being advected out of the Beaufort Sea (Howell et al., 2016), which has led to younger ice recirculating within the Gyre (Hutchings & Rigor, 2012) and all but eliminated the supply of MYI to the Eastern Arctic, which has predominantly been covered by seasonal ice since 2007 (Figure 1c; Kwok, 2018).

Based on increased MYI loss in the Beaufort Sea during the early-2000s Maslanik et al. (2007) proposed that the previously continuous journey of MYI through the Beaufort Gyre had been severed and that the western Arctic had become an area of MYI export. In this paper we use 25 years of Canadian Ice Service (CIS) ice charts to present an MYI budget for the Beaufort Sea that accounts for MYI transport and quantifies the annual area of MYI lost to melt in the region from 1997 to 2021. We then examine the thermodynamic forcing and dynamic conditioning that is driving the increase in MYI loss and examine MYI loss in the Beaufort Sea relative to MYI export through other pathways. Ultimately, we examine whether MYI transport through the Beaufort Gyre has been severed, leaving the Beaufort Sea as an area of MYI export.

2. Methods

To examine the MYI budget of the Beaufort Sea, the region was defined by four boundaries; (a) western (150°W), (b) northern (76.25°N), (c) M'Clure Strait, and (d) Amundsen Gulf (Figure 1d). The regional MYI area was calculated from ice charts and used to calculate the seasonal change in MYI area during summer (ΔMYI_S ; May through September) and winter (ΔMYI_W ; October through April), while MYI flux (F) across the boundaries was calculated from ice charts and remotely sensed fields of sea ice motion. ΔMYI_W is solely the result of F , while a combination of F and melt dictate ΔMYI_S . Therefore, by calculating the net F during summer we estimate the annual area of MYI lost to melt. MYI area may also be reduced through ice deformation; however, following Kwok and Cunningham (2010) this is expected to be very low and is not considered in this budget. The final term in the budget is local MYI replenishment from FYI that survives through summer and becomes classified as MYI on October 1. MYI replenishment is quantified as the regional FYI area in the ice chart from the week prior to October 1.

Ice charts delineate different ice regimes with polygons that present the partial concentrations (tenths) of up to three different stages of development according to the World Meteorological Organizations egg code (Fequet, 2005). Since 1996, ice charts are created by manually classifying these polygons in RADARSAT images. Within this study we focus on the partial concentration of MYI, which is distinguished from the surrounding FYI types by the tone, texture, and shape within the images (Tivy et al., 2011). Historically, ice charts were produced weekly during summer and either bi-weekly or monthly during winter. Since 2007 ice charts have been produced weekly year-round. Overall, ice charts provide a consistent, long-term evaluation of the partial concentration of MYI at high resolutions. The ice charts are considered more accurate than coarser pan-Arctic fields of ice age derived from lagrangian ice tracking (NSIDC Ice Age; Tschudi et al., 2019a) and provide year-round data unlike ice type data sets that are only available seasonally (OSI SAF Sea Ice Type; osi-saf.eumetsat.int). Further details on the ice charts and associated uncertainties are discussed in Tivy et al. (2011).

F was calculated at regular intervals along the western (F_W), northern (F_N), and M'Clure (F_M) boundaries using the following equation,

$$F = c_{MYI} u \Delta x \quad (1)$$

where c_{MYI} is the partial MYI concentration from the ice chart for the corresponding week/month, u is the daily ice velocity component normal to the gate, and Δx is the distance interval (5 km). F was not calculated for the Amundsen Gulf because during our study period, it was predominantly covered by FYI (Galley et al., 2016). F_W and F_N were calculated daily using the corresponding ice chart to assess c_{MYI} at each point and u from the NSIDC's Polar Pathfinder ice motion data set (v4; Tschudi et al., 2019b). However, this data set does not cover the narrow channels of the CAA; hence, a finer resolution sea ice motion data set derived from sequential RADARSAT images (described in Howell & Brady, 2019) was used in conjunction with the ice charts to quantify monthly values of F_M . Note that F_M is null from November to April due to landfast ice conditions in the M'Clure Strait (Canadian Ice Service, 2011). Across all three gates, positive fluxes represent ice import into the Beaufort Sea

and vice versa for negative fluxes. Summing F_N , F_W , and F_M provided the net seasonal F during summer (1 May to 30 September) and winter (1 October to 30 April), with the former being used to calculate the annual MYI area lost to melt.

The uncertainty in these estimates of MYI lost to melt reflect the uncertainty in F , which can be estimated with the following equation,

$$\sigma_F = \sigma_e L / \sqrt{N} \quad (2)$$

where, σ_e is the error in ice drift velocities (km d^{-1}), L is the gate width (km), and N is the number of samples across the gate. Using this equation and $\sigma_e = 0.43 \text{ km d}^{-1}$, Howell et al. (2013) calculated the uncertainty of F_M as $13 \text{ km}^2 \text{ d}^{-1}$. σ_e for the NSIDC ice drift velocities is greater and increases from 0.873 km d^{-1} between November and April to 1.123 km d^{-1} between May and October (Sumata et al., 2014). Additionally, σ_e increases with drift speed (Sumata et al., 2015), which may lead to a bias in underestimating ice flux during periods of high ice drift speeds. With values of L and N of 715 km and 143 samples for the northern gate and 635 km and 127 samples for the western gate, the uncertainty in F_N and F_W are 67 and $63 \text{ km}^2 \text{ d}^{-1}$ during summer and 52 and $49 \text{ km}^2 \text{ d}^{-1}$ during winter. During summer (May 1–September 30) this equates to cumulative σ_F in F_N , F_W , and F_M of 10,184, 9,576, and $1,976 \text{ km}^2$, respectively, or an overall σ_F of $21,736 \text{ km}^2$, which is approximately 17% of the average MYI loss ($125,000 \text{ km}^2$). However, MYI is not present along the entire gate at all times, so σ_F is lower. Calculating σ_F daily only for points along the northern and western boundaries where MYI is present, and summing over the melt season, along with σ_F in F_m , gives an average revised σ_F of $18,575 \text{ km}^2$ or 15% of the average MYI loss.

To complement the MYI budget, several additional data sets were used. The NSIDC Sea Ice Age data set (v4 - Tschudi et al., 2019a) provides context on the age distribution of MYI within the Beaufort Sea at the end of winter and was used to calculate a second MYI budget that confirms the overall trend of increasing MYI loss in the Beaufort Sea, albeit with a greater magnitude ($-10,000 \text{ km}^2 \text{ yr}^{-1}$; Figure S1 in Supporting Information S1). The Pan-Arctic Ice-Ocean Modeling and Assimilation System (PIOMAS; Zhang & Rothrock, 2003) provided estimates of ice thickness along the northern and western boundaries of the Beaufort Sea. Additionally, six hourly fields of 2 m air temperature and surface solar radiation downwards (SSRD) were retrieved from the ERA-5 reanalysis (Hersbach et al., 2020). Following Perovich et al. (2007, 2008), SSRD was used in combination with daily fields of sea ice concentration (Cavalieri et al., 1996; updated 2021) to estimate solar heating of the upper ocean through areas of open water (F_{ow}). F_{ow} is strongly correlated with bottom melt through the ice-albedo feedback and is associated with both the long-term increase in bottom melt and years of anomalously high ice loss in the Beaufort Sea (Babb et al., 2016, 2019; Perovich et al., 2008, 2011; Planck et al., 2020).

3. Results and Discussion

3.1. Regional MYI Budget

From 1997 to 2021 there has been a significant negative trend in the MYI area in the Beaufort Sea at the start of May ($-3,805 \text{ km}^2 \text{ yr}^{-1}$) and end of September ($-5,561 \text{ km}^2 \text{ yr}^{-1}$; Figure 2a). The trend in September is $\sim 35\%$ greater than the trend in May, highlighting the tendency toward greater reductions in the MYI area during summer and the continued replenishment of MYI via import during winter, which offsets MYI loss from the previous summer (i.e., 2013 and 2018; Figure 2b). Other than import, MYI area can only increase by local MYI replenishment, a process that has been fairly limited over this 25-year period (mean = $28,850 \text{ km}^2$) with the exception of 2013 (Figure 2b).

In terms of MYI transport, the net seasonal MYI flux varies considerably between years according to the balance of western export and northern import, with transport through the M'Clure Strait accounting for only 10% of the summer MYI flux (Figure 2). During winter the average net MYI flux is an export of $4,490 \text{ km}^2$, but there is considerable interannual variability between import and export. For example, winter export peaked at $245,000 \text{ km}^2$ in 1998 and preconditioned low ice conditions that summer (Maslanik et al., 1999), while winter import peaked at $183,500 \text{ km}^2$ in 2013 and replenished MYI in the Beaufort Sea following the complete loss of the Beaufort ice pack in summer 2012 (Babb et al., 2016, Figure 2c). Underlying the variability in MYI fluxes during winter is a significant positive trend in MYI import ($6,315 \text{ km}^2 \text{ yr}^{-1}$) that has flipped winter from a period of MYI export at the start of the time series to a period of MYI import and replenishment more recently (Figure 2c).

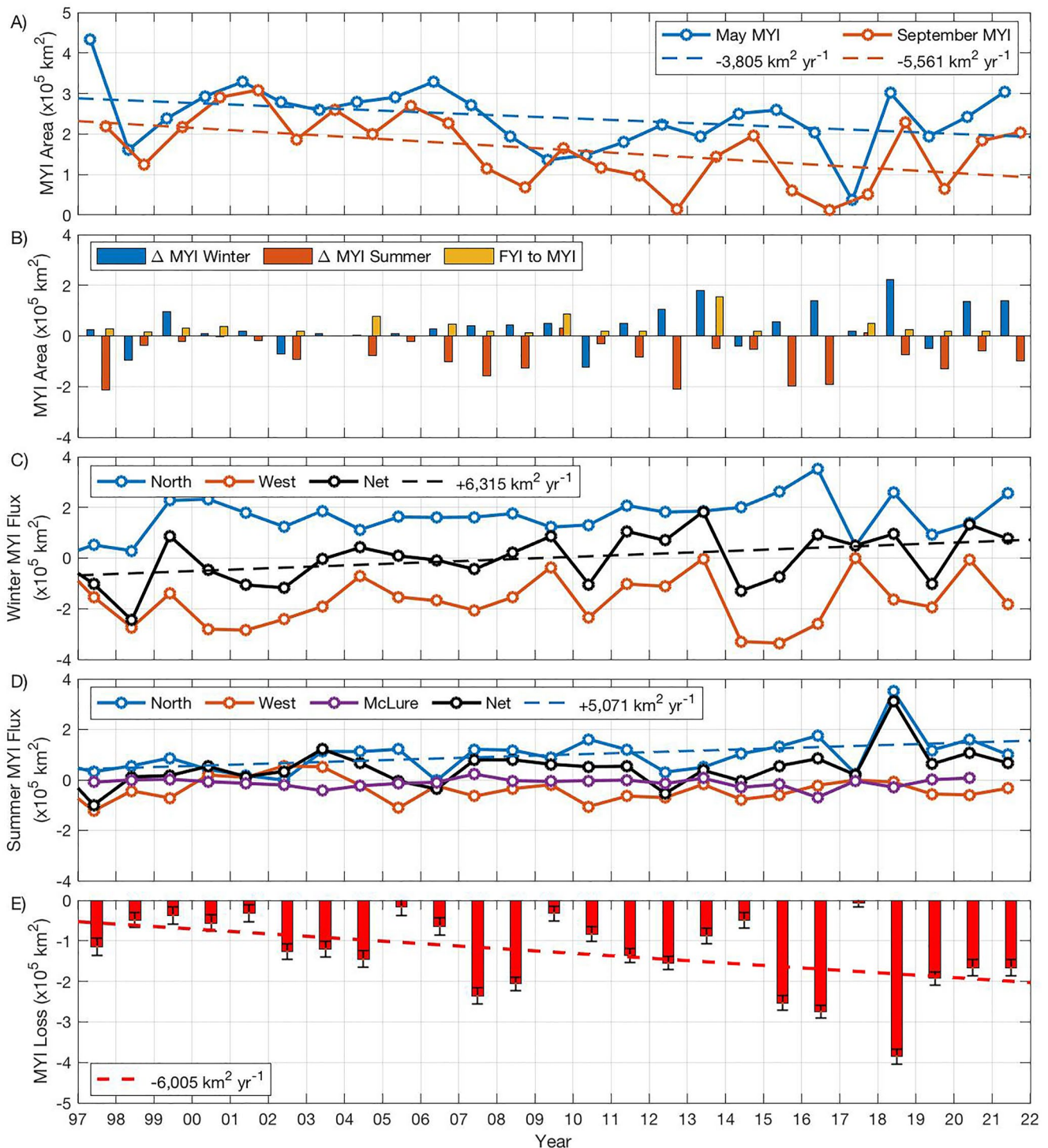


Figure 2. Annual time series of the MYI budget from 1997 to 2021. (a) Regional MYI area during May and September. (b) Seasonal changes in MYI area during winter and summer, and MYI replenishment during October. Seasonal MYI fluxes during winter (c) and summer (d) across the northern, western, and M'Clure boundaries along with the net seasonal MYI flux. (e) MYI area loss in the Beaufort Sea with associated error bars. Dashed lines denote significant ($p < 0.05$) trends.

During summer, an average of 47,120 km² of MYI is imported into the Beaufort Sea (Figure 2d). Summer export peaked at 99,430 km² in 1997 and contributed to the dramatic regional loss of MYI prior to the 1998 minimum, while summer import peaked at 312,670 km² in 2018 and was solely the result of northern import. From 1997

to 2021, there has been a significant positive trend in northern MYI import during summer ($5,071 \text{ km}^2 \text{ yr}^{-1}$; Figure 2d).

Overall, from 1997 to 2021, MYI transport through the Beaufort Sea was highly variable, but significant trends toward greater MYI import year-round have been loading MYI from the central Arctic into the Beaufort. However, less of this MYI is surviving through summer. From 1997 to 2021, an average of $125,000 \text{ km}^2$ of MYI area was lost in the Beaufort Sea each summer. The minimum loss occurred in 2017, when very little MYI was present in the Beaufort following the reversal of the Beaufort Gyre (Babb et al., 2020), while the maximum loss ($385,000 \text{ km}^2$) occurred in 2018, though record northern import maintained a peak in regional MYI area during September 2018 (Figure 2). Between 1997 and 2021, there was a significant increase in MYI loss in the Beaufort Sea ($-6,005 \text{ km}^2 \text{ yr}^{-1}$; Figure 2e). The fact that the trends in MYI loss and September MYI area ($-5,561 \text{ km}^2 \text{ yr}^{-1}$) are similar, coupled with a nonsignificant trend in net MYI transport during summer indicates that melt, not transport, is driving the increase in MYI loss in the Beaufort Sea.

3.2. Thermodynamic Forcing and Dynamic Conditioning of MYI Loss

MYI loss is not a new phenomenon in the Beaufort Sea, though between 1981 and 2005 only 7% of MYI in the western Arctic melted out each summer (Maslanik et al., 2011). The recent increase in MYI loss reflects a balance of factors that either drive ice melt (i.e., air temperatures and the ice-albedo feedback) or dictate the condition and therefore the resiliency of the ice pack entering the melt season (i.e., thickness and age). Examining these factors over the same period as the budget reveals nonsignificant increases in air temperatures and F_{ow} during summer, with notable peaks during years of regional sea ice minima (1998, 2008, 2012, and 2016; Figure 3) during which MYI loss also peaked (Figure 2e). At the same time, the presence of MYI in the Beaufort Sea has not only declined but the age of the MYI has decreased, with a dramatic loss of MYI 5+ years old since 2010 (Figure 3c). This accompanies a negative trend in ice thickness along the northern gate during both winter and summer (Figure 3d). Interestingly, the peak in MYI loss during 2018 does not correspond to anomalously warm air temperatures or increased F_{ow} during summer but rather to an end-of-winter ice pack that was very young, with a majority of the MYI being only 2 years old (Figure 3) and in part created by low ice conditions during the two preceding summers (Babb et al., 2019; 2020). Overall, the Beaufort ice pack has been getting progressively younger, thinner, and therefore less resilient, while it has also been exposed to warmer air temperatures and a stronger ice-albedo feedback.

3.3. Has MYI Loss Severed MYI Transport Within the Beaufort Gyre?

From 1997 to 2020, an average of $200,000 \text{ km}^2$ of MYI was exported from the Beaufort Sea across the western gate annually. However, western export is highly variable and ranged from a maximum export of $406,000 \text{ km}^2$ in 2014 following the recovery of MYI in 2013 to a net import of 750 km^2 in 2017 as a result of the Beaufort Gyre reversal (Babb et al., 2020). Strong variability in MYI export precludes significant trends, although during four recent winters essentially no MYI was exported across the gate (2009, 2013, 2017, and 2020; Figure 2c). Furthermore, there is a significant positive trend in FYI export across the western gate ($11,300 \text{ km}^2 \text{ yr}^{-1}$), indicating younger ice is being exported into the Chukchi Sea in place of MYI.

While there has not been a significant trend in MYI export across the western gate, there has been a decrease in the thickness and physical character of MYI exported across the gate. At the end of summer 2009, the remnant MYI in the western Beaufort Sea was heavily deteriorated and isothermal (Barber et al., 2009), while since 2007 remnant MYI has been so thin that by the end of the following winter, it is as thick as the surrounding FYI (Mahoney et al., 2019). Furthermore, there are significant negative trends in sea ice thickness along the western gate during summer and winter that equate to approximately 1.5 m over the study period (Figure 3).

MYI transport through the Beaufort Sea as part of the Beaufort Gyre has not been totally severed. However, it has been interrupted and reductions in the area, thickness, and age of MYI transported downstream into the Chukchi Sea have made that ice pack more vulnerable to warm Pacific waters flowing through the Bering Strait (Woodgate et al., 2010) and the ice-albedo feedback (Serreze et al., 2016).

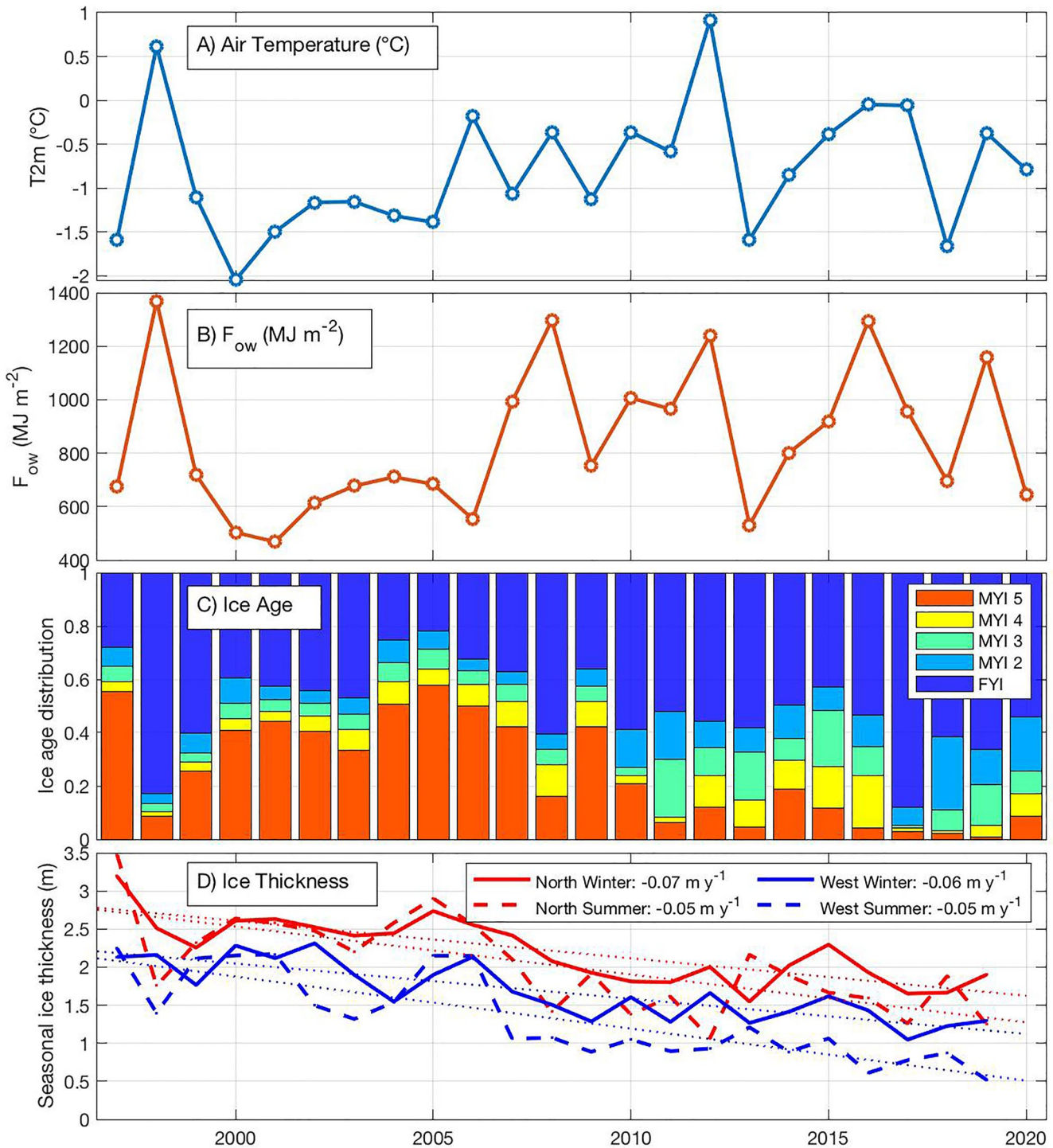


Figure 3. Time series of the thermodynamic and dynamic factors that either drive melt or condition the ice pack. Mean air temperature (a) and cumulative F_{ow} (b) over the Beaufort Sea from May through September. (c) Distribution of ice age within the Beaufort Sea at the end of April. (d) Mean seasonal ice thickness along the northern and western boundaries during winter and summer. Significant trends ($p < 0.05$) are presented with dotted lines.

3.4. Has the Beaufort Sea Become an Area of MYI Export?

Traditionally, MYI export occurs along the boundaries of the Arctic Ocean and represents the total loss of MYI. The Fram Strait is the primary export pathway (Kwok, 2009) exporting between 450,000 and 660,000 km² of MYI annually (Table 1). MYI is also exported annually through Nares Strait and into the Queen Elizabeth Islands

Table 1
Comparison of MYI Loss in the Beaufort Sea to MYI Export Through Export Pathways

	Years	Annual MYI loss		
MYI loss in the Beaufort Sea	1997–2001	42,360 km ²		
	2017–2021	183,250 km ²		
Export pathway	Years	Annual ice export	Proportion MYI	Annual MYI loss
Fram strait	1979–2007	706,000 km ^{2a}	64%–94% ^b	451,000–663,000 km ²
Nares strait	1996–2002	33,000 km ^{2c}	50% ^c	16,500 km ²
	2019–2021	87,000 km ^{2d}	50% ^c	43,500 km ²
QEI	1997–2002	8,000 km ^{2e}	100% ^g	8,000 km ²
	1997–2018	25,000 km ^{2f}	100% ^g	25,000 km ²

^aKwok (2009). ^bRicker et al., (2018). ^cKwok, (2005). ^dMoore et al., (2021). ^eKwok, (2006). ^fHowell & Brady (2019). ^gEstimated based on the CIS ice charts.

(QEI; Howell & Brady, 2019; Kwok, 2005; 2006; Moore et al., 2021) and has occasionally been exported into the Barents Sea (Kwok, 2004) and through the Bering Strait (Babb et al., 2013). In order to define the Beaufort Sea as an export pathway similar to these other locations, the regional MYI pack would have to be completely lost. This has happened three times during the last decade (2010, 2012, and 2016). But as we have just shown, younger and thinner MYI does continue to be advected downstream within the Gyre. Hence, the Beaufort Sea has not completely become an export pathway, but it increasingly resembles one.

Comparing MYI loss in the Beaufort to MYI export through the traditional export pathways reveals that during the first pentad of our budget (1997–2001) MYI loss in the Beaufort was approximately twice the net MYI export through the Nares Strait and into the QEI but only 6%–9% of the MYI export through the Fram Strait (Table 1). Comparatively, during the most recent pentad (2017–2021), MYI loss in the Beaufort Sea was approximately three times the net MYI export through the Nares Strait and into the QEI, and approximately 27%–40% of the annual MYI export through the Fram Strait (Table 1). Furthermore, the 2018 peak in MYI loss (385,000 km²) was close to the conservative estimate of MYI export through the Fram Strait.

Without estimates of MYI loss in other regions, it is not possible to compare subregional MYI loss to the overall pan-Arctic annual MYI loss (melt + export). Although this comparison shows that among these four pathways of MYI loss, the Beaufort Sea continues to have the second greatest magnitude and that its relative contribution to the Arctic MYI balance has significantly increased. This increase is critical for the MYI that remains in the central Arctic, as it is now bookended by the Fram Strait and Beaufort Sea (Figure 1) and is susceptible to being lost through either side. Historically, MYI advected from the central Arctic through the Beaufort Gyre was conserved, particularly during a negative phase of the Arctic oscillation when a large Beaufort Gyre retained ice within the western Arctic (Rigor et al., 2002; Stroeve et al., 2011). However, increasing MYI loss in the Beaufort Sea limits the potential of the Gyre to retain MYI and facilitate a recovery. As an example, during winter 2021, a strong Beaufort High advected MYI out of the central Arctic into the Beaufort Sea (Mallett et al., 2021), and while this facilitated a slight recovery in the regional MYI area (Figure 2a), over 170,000 km² of this MYI was lost (Figure 2e) and we speculate that the remaining MYI was heavily deteriorated.

Ultimately, the combination of increasing MYI loss in the Beaufort Sea (Figure 2e), increasing MYI export through the Nares Strait (Moore et al., 2021) and into the QEI (Howell & Brady, 2019), and continued MYI export through the Fram Strait is depleting the reservoir of MYI in the Arctic Ocean. This trend is compounded by a concomitant decrease in MYI replenishment by FYI (Kwok, 2007). The imbalance between MYI loss (melt and export) and MYI replenishment from FYI is driving the transition to a predominantly seasonal ice cover that is inherently thinner and will eventually lead to the occurrence of a seasonally ice-free Arctic (SIMIP, 2020).

3.5. The Impacts of Increasing MYI Loss in the Beaufort Sea

The loss of MYI has various impacts on the way that humans and wildlife interact with the ice pack within the Beaufort Sea. Given its thickness and strength, MYI represents a considerable hazard to vessels operating in

ice-covered waters. The reduction in MYI area within the Beaufort Sea corresponds to an increase in shipping activity (Pizzolato et al., 2016), particularly pleasure crafts that are accessing the Northwest Passage (Dawson et al., 2018). Shipping in the Beaufort Sea is proposed to continue to increase as the shipping season length continues to increase (Mudryk et al., 2021). However, the continued replenishment of MYI during winter will maintain some level of risk associated with hazardous ice (Barber et al., 2014).

The transition to a thinner seasonal ice pack is projected to increase productivity in the Arctic (Tedesco et al., 2019) and has been proposed to offer some short-term benefits to Polar bears (Derocher et al., 2004). However, Laidre et al. (2020) noted that this has yet to be demonstrated and suggest any advantage may only be temporary before the negative effects of climate change (i.e., habitat loss) begin to outweigh any potential positives. Historically, Polar bears within the Beaufort Sea retreated to the MYI pack during summer (Derocher et al., 2004) and even denned on MYI floes during winter (Amstrup & Gardner, 1994). But MYI loss combined with the northern retreat of the MYI edge (Galley et al., 2016) is both removing and fragmenting this habitat and increasing the distance that bears may need to swim to reach either the remaining MYI or land (Pagano et al., 2021).

4. Conclusions

Historically, the Beaufort Sea served as a conduit for MYI transport from the central Arctic to the Eastern Arctic through the Beaufort Gyre, and thereby facilitated the pan-Arctic distribution of MYI. However, increasing ice melt during the early 2000s led Maslanik et al. (2007) to propose that the Beaufort Sea had become an area of MYI export and that MYI transport through the Beaufort Gyre had been severed. Using a regional MYI budget from 1997 to 2021, we determined that MYI transport through the Beaufort Sea has not been completely severed, but that it has been interrupted and essentially now provides no replenishment of MYI to the Eastern Arctic. The budget reveals that MYI import into the Beaufort Sea has increased during both summer and winter, but that less of this MYI now survives through summer. Over the 25-year study period, MYI area loss increased at $6,289 \text{ km}^2 \text{ yr}^{-1}$, nearly quadrupling the annual mean area of MYI lost from $42,360 \text{ km}^2$ between 1997 and 2001 to $183,000 \text{ km}^2$ between 2017 and 2021. MYI area loss peaked at $385,000 \text{ km}^2$ in 2018.

Historically, the pan-Arctic MYI budget was dominated by MYI loss through the Fram Strait. At the start of the record, MYI loss in the Beaufort Sea represented only 7% of the annual MYI export through the Fram Strait. However, from 2017 to 2021, this increased to $\sim 35\%$, with the peak in 2018 matching the conservative estimate of MYI export through the Fram Strait ($\sim 400,000 \text{ km}^2$). This increase in MYI loss in the Beaufort Sea has been driven by a combination of thermodynamic forcing and dynamic conditioning, which has collectively exposed a younger, thinner ice pack to warmer air temperatures and a stronger ice-albedo feedback. Increased MYI loss has interrupted MYI transport through the Gyre, leading to a deteriorated form of MYI being advected downstream. Ultimately, the contribution of MYI loss in the Beaufort Sea to the overall MYI budget of the Arctic Ocean has dramatically increased and is a key driver of the transition to a seasonal Arctic ice pack.

Acknowledgments

Tragically D. Barber passed away shortly after this paper was accepted; he was a giant in Arctic research and will be remembered as such. D. Babb, R. Galley, and D. Barber would like to acknowledge the financial support from the Natural Sciences and Engineering Research Council of Canada (NSERC). Thanks to the Canada Research Chair (CRC), Canada Excellence Research Chair (CERC), and the Canada-150 Chair (C-150) programs. D. Babb acknowledges financial support from the Canadian Meteorological and Oceanographic Society (CMOS). J. Landy acknowledges support from the Centre for Integrated Remote Sensing and Forecasting for Arctic Operations (CIRFA) project through the Research Council of Norway (RCN) under grant #237906. J. Landy and J. Stroeve acknowledge support from the Natural Environment Research Council Project "PRE-MELT" under Grant No. NE/T000546/1. We would also like to thank the editor and two anonymous reviewers for their help in improving this manuscript.

Data Availability Statement

CIS ice charts are freely available online (<https://www.canada.ca/en/environment-climate-change/services/ice-forecasts-observations.html>). The NSIDC ice motion (<https://nsidc.org/data/nsidc-0116/versions/4>) and ice age (<https://nsidc.org/data/NSIDC-0611/versions/4>) data sets are available online. PIOMAS Ice thickness data are available online (http://psc.apl.uw.edu/research/projects/arctic-sea-ice-volume-anomaly/data/model_grid). ERA5 atmospheric reanalysis products are available from the Climate Data Store through the Copernicus Climate Change Service (<https://cds.climate.copernicus.eu/cdsapp#!/dataset/reanalysis-era5-single-levels?tab=overview>).

References

- Amstrup, S. C., & Gardner, C. L. (1994). Polar bear maternity denning in the Beaufort Sea. *Journal of Wildlife Management*, 58(1), 1–10. <https://doi.org/10.2307/3809542>
- Babb, D. G., Galley, R. J., Asplin, M. G., Lukovich, J. V., & Barber, D. G. (2013). Multiyear sea ice export through the Bering Strait during winter 2011–2012. *Journal of Geophysical Research: Oceans*, 118(10), 5489–5503. <https://doi.org/10.1002/jgrc.20383>
- Babb, D. G., Galley, R. J., Barber, D. G., & Rysgaard, S. (2016). Physical processes contributing to an ice free Beaufort Sea during September 2012. *Journal of Geophysical Research: Oceans*, 121(1), 267–283. <https://doi.org/10.1002/2015JC010756>

- Babb, D. G., Landy, J. C., Barber, D. G., & Galley, R. J. (2019). Winter sea ice export from the Beaufort Sea as a preconditioning Mechanism for enhanced summer melt: A Case study of 2016. *Journal of Geophysical Research: Oceans*, 1998(6575), 6575–6600. <https://doi.org/10.1029/2019JC015053>
- Babb, D. G., Landy, J. C., Lukovich, J. V., Haas, C., Hendricks, S., Barber, D. G., & Galley, R. J. (2020). The 2017 reversal of the Beaufort Gyre: Can dynamic thickening of a seasonal ice cover during a reversal limit summer ice melt in the Beaufort Sea? *Journal of Geophysical Research: Oceans*, 125(12), 1–26. <https://doi.org/10.1029/2020jc016796>
- Barber, D. G., Galley, R. J., Asplin, M. G., De Abreu, R., Warner, K. A., Pučko, M., et al. (2009). Perennial pack ice in the southern beaufort sea was not as it appeared in the summer of 2009. *Geophysical Research Letters*, 36(24), 1–5. <https://doi.org/10.1029/2009GL041434>
- Barber, D. G., McCullough, G., Babb, D. G., Komarov, A., Candlish, L. M., Lukovich, J. V., et al. (2014). Climate change and ice hazards in the Beaufort Sea. *Elementa: Science of the Anthropocene*, 2(1982), 000025. <https://doi.org/10.12952/journal.elementa.000025>
- Bourke, R. H., & Garret, R. P. (1987). Sea ice thickness distribution in the Arctic Ocean. *Cold Regions Science and Technology*, 13(3), 259–280. [https://doi.org/10.1016/0165-232x\(87\)90007-3](https://doi.org/10.1016/0165-232x(87)90007-3)
- Canadian Ice Service. (2011). *Sea ice climatic Atlas for the northern Canadian waters 1981-2011*.
- Cavalieri, D. J., Parkinson, C. L., Gloersen, P., & Zwally, H. J. (1996). *Sea ice concentrations from Nimbus-7 SMMR and DMSP SSM/I-SSM/I Passive Microwave data*.
- Dawson, J., Pizzolato, L., Howell, S. E. L., Copland, L., & Johnston, M. E. (2018). Temporal and Spatial patterns of ship Traffic in the Canadian Arctic from 1990 to 2015 + Supplementary Appendix 1: Figs. S1–S7 (See Article Tools). *Arctic*, 71(1), 15. <https://doi.org/10.14430/arctic4698>
- Derocher, A. E., Lunn, N. J., & Stirling, I. (2004). Polar bears in a warming climate. *Integrative and Comparative Biology*, 44(2), 163–176. <https://doi.org/10.1093/icb/44.2.163>
- Fequet, D. (2005). *Manual of standard Procedures for observing and reporting ice conditions* (9th ed.). Canadian Ice Service.
- Galley, R. J., Babb, D. G., Ogi, M., Else, B. G. T., Geifus, N. X., Crabeck, O., et al. (2016). Replacement of multiyear sea ice and changes in the open water season duration in the Beaufort Sea since 2004. *Journal of Geophysical Research: Oceans*, 121(April), 1–18. <https://doi.org/10.1002/2015JC011583>. Received
- Hersbach, H., Bell, B., Berrisford, P., Hirahara, S., Horányi, A., Muñoz-Sabater, J., et al. (2020). The ERA5 global reanalysis. *Quarterly Journal of the Royal Meteorological Society*, 146(730), 1999–2049. <https://doi.org/10.1002/qj.3803>
- Howell, S. E. L., & Brady, M. (2019). The dynamic response of sea ice to warming in the Canadian Arctic Archipelago. *Geophysical Research Letters*, 46(22), 13119–13125. <https://doi.org/10.1029/2019GL085116>
- Howell, S. E. L., Brady, M., Derksen, C., & Kelly, R. E. J. (2016). Recent changes in sea ice area flux through the Beaufort Sea during the summer. *Journal of Geophysical Research: Oceans*, 121(4), 1–14. <https://doi.org/10.1002/2015JC011464>
- Howell, S. E. L., Wohlleben, T., Dabboor, M., Derksen, C., Komarov, A., & Pizzolato, L. (2013). Recent changes in the exchange of sea ice between the Arctic Ocean and the Canadian Arctic Archipelago. *Journal of Geophysical Research: Oceans*, 118(7), 3595–3607. <https://doi.org/10.1002/jgrc.20265>
- Hutchings, J. K., & Rigor, I. G. (2012). Role of ice dynamics in anomalous ice conditions in the Beaufort Sea during 2006 and 2007. *Journal of Geophysical Research*, 117(5), 1–14. <https://doi.org/10.1029/2011JC007182>
- Krishfield, R. A., Proshutinsky, A., Tateyama, K., Williams, W. J., Carmack, E. C., McLaughlin, F. A., & Timmermans, M.-L. (2014). Deterioration of perennial sea ice in the Beaufort Gyre from 2003 to 2012 and its impact on the oceanic freshwater cycle. *Journal of Geophysical Research: Oceans*, 119(2), 35–1305. <https://doi.org/10.1002/2013JC008999>
- Kwok, R. (2004). Fram strait sea ice outflow. *Journal of Geophysical Research*, 109(C1), C01009. <https://doi.org/10.1029/2003JC001785>
- Kwok, R. (2005). Variability of Nares Strait ice flux. *Geophysical Research Letters*, 32(24), 1–4. <https://doi.org/10.1029/2005GL024768>
- Kwok, R. (2006). Exchange of sea ice between the Arctic Ocean and the Canadian Arctic Archipelago. *Geophysical Research Letters*, 33(16), 1–5. <https://doi.org/10.1029/2006GL027094>
- Kwok, R. (2007). Near zero replenishment of the Arctic multiyear sea ice cover at the end of 2005 summer. *Geophysical Research Letters*, 34(5), 1–6. <https://doi.org/10.1029/2006GL028737>
- Kwok, R. (2009). Outflow of Arctic Ocean sea ice into the Greenland and Barent seas: 1979-2007. *Journal of Climate*, 22(9), 2438–2457. <https://doi.org/10.1175/2008JCLI2819.1>
- Kwok, R. (2015). Sea ice convergence along the Arctic coasts of Greenland and the Canadian Arctic Archipelago: Variability and extremes (1992-2014). *Geophysical Research Letters*, 42(18), 1–8. <https://doi.org/10.1002/2015GL065462>
- Kwok, R. (2018). Arctic sea ice thickness, volume, and multiyear ice coverage: Losses and coupled variability (1958 – 2018). *Environmental Research Letters*, 13(10), 105005. <https://doi.org/10.1088/1748-9326/aae3ec>
- Kwok, R., & Cunningham, G. F. (2010). Contribution of melt in the Beaufort Sea to the decline in Arctic Multiyear sea ice coverage: 1993-2009. *Geophysical Research Letters*, 37(20), 1–5. <https://doi.org/10.1029/2010GL044678>
- Laidre, K. L., Atkinson, S. N., Regehr, E. V., Stern, H. L., Born, E. W., Wiig, Ø., et al. (2020). Transient benefits of climate change for a high-Arctic polar bear (*Ursus maritimus*) subpopulation. *Global Change Biology*, 26(11), 6251–6265. <https://doi.org/10.1111/gcb.15286>
- Mahoney, A. R., Hutchings, J. K., Eicken, H., & Haas, C. (2019). Changes in the thickness and circulation of multiyear ice in the beaufort Gyre determined from Pseudo-Lagrangian methods from 2003–2015. *Journal of Geophysical Research: Oceans*, 124(8), 5618–5633. <https://doi.org/10.1029/2018JC014911>
- Mallett, R. D. C., Stroeve, J. C., Cornish, S. B., Crawford, A. D., Lukovich, J. V., Serreze, M. C., et al. (2021). Record winter winds in 2020/21 drove exceptional Arctic sea ice transport. *Communications Earth & Environment*, 2(1), 17–22. <https://doi.org/10.1038/s43247-021-00221-8>
- Maslanik, J. A., Fowler, C., Stroeve, J. C., Drobot, S., Zwally, J., Yi, D., & Emery, W. (2007). A younger, thinner Arctic ice cover: Increased potential for rapid, extensive sea-ice loss. *Geophysical Research Letters*, 34(24), 2004–2008. <https://doi.org/10.1029/2007GL032043>
- Maslanik, J. A., Serreze, M. C., & Agnew, T. (1999). On the record reduction in 1998 Western Arctic sea-ice cover. *Geophysical Research Letters*, 26(13), 1905–1908. <https://doi.org/10.1029/1999GL900426>
- Maslanik, J. A., Stroeve, J. C., Fowler, C., & Emery, W. (2011). Distribution and trends in Arctic sea ice age through spring 2011. *Geophysical Research Letters*, 38(13), 2–7. <https://doi.org/10.1029/2011GL047735>
- Moore, G. W. K., Howell, S. E. L., Brady, M., Xu, X., & McNeil, K. (2021). Anomalous collapses of Nares Strait ice arches leads to enhanced export of Arctic sea ice. *Nature Communications*, 12(1), 1–8. <https://doi.org/10.1038/s41467-020-20314-w>
- Mudryk, L. R., Dawson, J., Howell, S. E. L., Derksen, C., Zagon, T. A., & Brady, M. (2021). Impact of 1, 2 and 4°C of global warming on ship navigation in the Canadian Arctic. *Nature Climate Change*, 11(8), 29–31. <https://doi.org/10.1038/s41558-021-01087-6>
- Nghiem, S. V., Rigor, I. G., Perovich, D. K., Clemente-Colón, P., Weatherly, J. W., & Neumann, G. (2007). Rapid reduction of Arctic perennial sea ice. *Geophysical Research Letters*, 34(19), 1–6. <https://doi.org/10.1029/2007GL031138>
- Pagano, A. M., Durner, G. M., Atwood, T. C., & Douglas, D. C. (2021). Effects of sea ice decline and summer land use on polar bear home range size in the Beaufort Sea. *Ecosphere*, 12(10). <https://doi.org/10.1002/ecs2.3768>

- Perovich, D. K., Nghiem, S. V., Markus, T., & Schweiger, A. (2007). Seasonal evolution and interannual variability of the local solar energy absorbed by the Arctic sea ice–ocean system. *Journal of Geophysical Research*, *112*, C03005. <https://doi.org/10.1029/2006JC003558>
- Perovich, D. K., Richter-Menge, J. A., Jones, K. F., & Light, B. (2008). Sunlight, water, and ice: Extreme Arctic sea ice melt during the summer of 2007. *Geophysical Research Letters*, *35*(11), 2–5. <https://doi.org/10.1029/2008GL034007>
- Perovich, D. K., Richter-Menge, J. A., Jones, K. F., Light, B., Elder, B. C., Polashenski, C., et al. (2011). Arctic sea-ice melt in 2008 and the role of solar heating. *Annals of Glaciology*, *52*(57 Part 2), 355–359. <https://doi.org/10.3189/172756411795931714>
- Pizzolato, L., Howell, S. E. L., Dawson, J., Laliberté, F., & Copland, L. (2016). The influence of declining sea ice on shipping activity in the Canadian Arctic. *Geophysical Research Letters*, *43*(23), 12146–12154. <https://doi.org/10.1002/2016GL071489>
- Planck, C. J., Perovich, D. K., & Light, B. (2020). A Synthesis of observations and Models to assess the time series of sea ice mass balance in the Beaufort Sea. *Journal of Geophysical Research: Oceans*, *125*(11), 1–15. <https://doi.org/10.1029/2019jc015833>
- Ricker, R., Girard-Arduin, F., Krumpen, T., & Lique, C. (2018). Satellite-derived sea ice export and its impact on Arctic ice mass balance. *The Cryosphere*, *12*(9), 3017–3032. <https://doi.org/10.5194/tc-12-3017-2018>
- Rigor, I. G., & Wallace, J. M. (2004). Variations in the age of Arctic sea-ice and summer sea-ice extent. *Geophysical Research Letters*, *31*(9), 2–5. <https://doi.org/10.1029/2004GL019492>
- Rigor, I. G., Wallace, J. M., & Colony, R. L. (2002). Response of sea ice to the Arctic oscillation. *Journal of Climate*, *15*, 2648–2663. [https://doi.org/10.1175/1520-0442\(2002\)015<2648:ROSITT>2.0](https://doi.org/10.1175/1520-0442(2002)015<2648:ROSITT>2.0)
- Serreze, M. C., Crawford, A. D., Stroeve, J. C., Barrett, A. P., & Woodgate, R. A. (2016). Variability, trends, and predictability of seasonal sea ice retreat and advance in the Chukchi Sea. *Journal of Geophysical Research: Oceans*, *121*(10), 7308–7325. <https://doi.org/10.1002/2016JC011977>
- SIMIP Community. (2020). Arctic sea ice in CMIP6. *Geophysical Research Letters*, *47*(10). <https://doi.org/10.1029/2019gl086749>
- Stroeve, J. C., Maslanik, J. A., Serreze, M. C., Rigor, I. G., Meier, W., & Fowler, C. (2011). Sea ice response to an extreme negative phase of the Arctic Oscillation during winter 2009/2010. *Geophysical Research Letters*, *38*(2), 1–6. <https://doi.org/10.1029/2010GL045662>
- Sumata, H., Kwok, R., Gerdes, R., Kauker, F., & Karcher, M. (2015). Uncertainty of Arctic summer ice drift assessed by high-resolution SAR data. *Journal of Geophysical Research: Oceans*, *120*(8), 5285–5301. <https://doi.org/10.1002/2015JC010810>
- Sumata, H., Lavergne, T., Girard-Arduin, F., Kimura, N., Tschudi, M. A., Kauker, F., et al. (2014). An intercomparison of Arctic ice drift products to deduce uncertainty estimates. *Journal of Geophysical Research: Oceans*, *119*(8), 4887–4921. <https://doi.org/10.1002/2013JC009724>
- Tedesco, L., Vichi, M., & Scoccimarro, E. (2019). Sea-ice algal phenology in a warmer Arctic. *Science Advances*, *5*(5). <https://doi.org/10.1126/sciadv.aav4830>
- Tivy, A., Howell, S. E. L., Alt, B., McCourt, S., Chagnon, R., Crocker, G., et al. (2011). Trends and variability in summer sea ice cover in the Canadian Arctic based on the Canadian Ice Service Digital Archive, 1960–2008 and 1968–2008. *Journal of Geophysical Research*, *116*(3), C03007. <https://doi.org/10.1029/2009JC005855>
- Tschudi, M. A., Meier, W. N., Stewart, J. S., Fowler, C., & Maslanik, J. A. (2019a). *EASE-grid sea ice age, Version 4*. <https://doi.org/10.5067/UTAV7490FEPB>
- Tschudi, M. A., Meier, W. N., Stewart, J. S., Fowler, C., & Maslanik, J. A. (2019b). *Polar Pathfinder daily 25 km EASE-Grid sea ice motion vectors, Version 4*. <https://doi.org/10.5067/INAWUWO7QH7B>
- Woodgate, R. A., Weingartner, T., & Lindsay, R. (2010). The 2007 Bering Strait oceanic heat flux and anomalous Arctic sea-ice retreat. *Geophysical Research Letters*, *37*(1), 1–5. <https://doi.org/10.1029/2009GL041621>
- Zhang, J., & Rothrock, D. A. (2003). Modeling global sea ice with a thickness and enthalpy distribution model in generalized curvilinear coordinates. *Monthly Weather Review*, *131*(5), 845–861. <https://doi.org/10.1175/1520-0493>